Cancer Research

Tissue Factor Induced by Epithelial–Mesenchymal Transition Triggers a Procoagulant State That Drives Metastasis of Circulating Tumor Cells

Morgane Bourcy[1], Meggy Suarez-Carmona[1], Justine Lambert[1], Marie-Emilie Francart[1], Hélène Schroeder[2], Céline Delierneux[3], Nicolas Skrypek[4,5], Erik W. Thompson[6], Guy Jérusalem[2], Geert Berx[4,5], Marc Thiry[7], Silvia Blacher[1], Brett G. Hollier[8], Agnès Noël[1], Cécile Oury[3], Myriam Polette[9], and Christine Gilles[1]

Abstract

Epithelial–mesenchymal transition (EMT) is prominent in circulating tumor cells (CTC), but how it influences metastatic spread in this setting is obscure. Insofar as blood provides a specific microenvironment for tumor cells, we explored a potential link between EMT and coagulation that may provide EMT-positive CTCs with enhanced colonizing properties. Here we report that EMT induces tissue factor (TF), a major cell-associated initiator of coagulation and related procoagulant properties in the blood. TF blockade by antibody or shRNA diminished the procoagulant activity of EMT-positive cells, confirming a functional role for TF in these processes. Silencing the EMT transcription factor ZEB1 inhibited both EMT-associated TF expression and coagulant activity, further strengthening the link between EMT and coagulation. Accordingly, EMT-positive cells exhibited a higher persistance/survival in the lungs of mice colonized after intravenous injection, a feature diminished by TF or ZEB1 silencing. In tumor cells with limited metastatic capability, enforcing expression of the EMT transcription factor Snail increased TF, coagulant properties, and early metastasis. Clinically, we identified a subpopulation of CTC expressing vimentin and TF in the blood of metastatic breast cancer patients consistent with our observations. Overall, our findings define a novel EMT–TF regulatory axis that triggers local activation of coagulation pathways to support metastatic colonization of EMT-positive CTCs. *Cancer Res; 76(14); 1–13. ©2016 AACR.*

Introduction

The contribution of epithelial-to-mesenchymal transitions (EMT) to CTCs biology has generated much interest (1–5). EMT indeed provides epithelial tumor cells with enhanced migratory, invasive, and survival abilities that participate in the liberation of CTCs into the circulation (1, 2, 4, 5). A variety of EMT-inducing extracellular signals and signaling pathways have been shown to converge on the expression of EMT transcription factors including the Snail and ZEB families, Twist, and E47 (6–8). These transcription factors directly or indirectly repress or activate a variety of EMT target genes to provide cells with enhanced migratory and invasive ability, enhanced resistance to apoptosis and senescence, and proangiogenic and proinflammatory activities. While their repressive activity on several epithelial genes has been shown to involve a direct binding to promoter regions, their ability to induce mesenchymal genes rather implicates indirect and often unknown mechanisms (6–9). Closely linking EMT to CTC, the expression of EMT mediators has been detected in CTCs in animal models (2, 10) and in subpopulations of CTCs isolated from cancer patients including breast cancer patients, where they associate with poor clinical parameters and to the particularly aggressive "triple-negative breast cancer" (TNBC) subtype (5, 11, 12). It has thus been suggested that CTCs expressing EMT features could represent a premetastatic population, socalled metastasis-initiating cells (MIC). Phenotyping CTCs and unravelling the mechanisms that enable them to accomplish early steps of the metastatic spread (i.e., survival in the bloodstream and early seeding in distant organs) are major challenges for cancer research today.

Increasing literature today supports the involvement of coagulation events in cancer progression (13, 14). The activation of coagulation has indeed long been correlated with malignancy and the beneficial impact of anticoagulants on cancer progression has been demonstrated in animal models (15–17) and evaluated in

[1]GIGA-Cancer, Laboratory of Tumor and Development Biology, University of Liège, Liège, Belgium. [2]CHU, Department of Medical Oncology, University of Liège, Liège, Belgium. [3]GIGA-Cardiovascular Sciences, Laboratory of Thrombosis and Hemostasis, University of Liège, Liège, Belgium. [4]Unit of Molecular and Cellular Oncology Lab, Inflammation Research Center, VIB, Ghent, Belgium. [5]Department of Biomedical Molecular Biology, Cancer Research Institute Ghent (CRIG), Ghent University, Ghent, Belgium [6]Institute of Health and Biomedical Innovation and School of Biomedical Sciences Translational Research Institute, Queensland University of Technology, Brisbane, Australia. [7]GIGA-Neurosciences, Unit of Cell and Tissue Biology, University of Liège, Liège, Belgium. [8]Australian Prostate Cancer Research Centre - Queensland, Institute of Health and Biomedical Innovation, School of Biomedical Sciences, Queensland University of Technology, Princess Alexandra Hospital, Translational Research Institute, Brisbane, Australia. [9]INSERM UMR-S 903, CHU, Biopathology Laboratory, University of Reims, Reims, France.

Note: Supplementary data for this article are available at Cancer Research Online (http://cancerres.aacrjournals.org/).

Corresponding Author: Christine Gilles, Laboratory of Tumor and Development Biology (LBTD), GIGA-Cancer, Pathology Tower, B23, +4 CHU Sart-Tilman, University of Liège, Liège 4000, Belgium. Phone: 324-366-2453; Fax: 324-366-2936; E-mail: cgilles@ulg.ac.be

doi: 10.1158/0008-5472.CAN-15-2263

clinical studies (18). More precisely in relation to early events facilitating metastasis, studies using experimental models of metastases have reported the rapid formation of fibrin-platelet rich microthrombi in lung arterioles after intravenous injection of mouse tumor cells (19, 20). Using mice with genetic defects in distal hemostatic factors (prothrombin and fibrinogen), Degen and colleagues have clearly shown that coagulation events facilitate metastasis (13, 21).

Tissue factor (TF), a membrane-associated glycoprotein, has emerged as the central player in the relationship between the hemostatic system and cancer progression (13, 14, 22–26). TF binds and activates coagulation factor FVII, which in turn triggers the downstream coagulation cascade leading to thrombin generation and clot formation. Early screening studies have identified TF as a differentially expressed gene in invasive cell lines such as MDA-MB-231 breast cancer cell line. Enhanced TF expression has also been found in a variety of solid tumors including breast cancers, in which it associates with decreased overall survival or shorter recurrence-free survival (26). TF is a downstream target of several oncogenic pathways (RAS, HER2, MET, SHH), of the loss of tumor suppressors such as PTEN or p53, and of transcriptional regulation by NFκB, AP-1, or Egr-1 transcription factors (24, 25). Adding to its expression at the cell surface, TF may also be released in microparticles harboring procoagulant activity (27). Experimental data point to a determinant role of TF in facilitating both tumor growth and metastasis, involving both coagulation-dependent and -independent mechanisms. Indeed, in addition to its role in coagulation, TF is directly involved, through its cytoplasmic tail, in signaling events that modulate several cellular processes such as adhesion and migration, apoptosis, and angiogenesis (22, 23, 26, 28).

We here explored the hypothesis that CTCs expressing EMT traits could express high levels of TF, and harbor enhanced procoagulant activity that could facilitate early metastasis.

Materials and Methods

Cell culture

Human breast cancer cell lines (MCF7, T47D, MDA-MB-468, and Hs578T) were obtained from the ATCC. MDA-MB-231 and A549 luciferase-expressing clones were purchased from Caliper Life Sciences. The breast cancer PMC42-LA subline was obtained from Dr. M.L. Ackland (Deakin University, Burwood, Australia; ref. 29). Fibroblasts were isolated by explant from normal human dermis. Human dermal lymphatic endothelial cells (HDLEC) were obtained from PromoCell. All cell lines were used within 10 passages after authentication (STR DNA typing, Leibniz-Institute DSMZ), were mycoplasma free, and were cultured in DMEM (Gibco) supplemented with 10% FCS. HDLEC were cultured in EGM2-MV medium (Lonza).

For EMT induction, inducible cell lines were treated for 48 hours with 20 ng/mL recombinant EGF (Sigma, E9644) or 5 ng/mL recombinant TGFβ (R&D Systems, 240-B).

For Snail induction in the doxycycline-inducible Snail system, cells were seeded and treated with 250 ng/mL doxycycline (Sigma, D9891) for different time periods. A description of MDA-MB-468-iSnail generation is provided in Supplementary Materials and Methods.

siRNA transfection

For ZEB1 and Snail siRNA transfection, cells were transfected for 48 hours with RNAiMax (Thermo Fisher Scientific, Invitrogen) and 20 nmol/L of the siRNA duplexes. For TF siRNA transfection in MDA-MB-468-iSnail, cells were transfected by electroporation. The siRNA sequences are listed in Supplementary Table S1.

shRNA transduction

MDA-MB-468 and MDA-MB-231 cells were transduced (GIGA-Viral vectors platform, University of Liège, Liège, Belgium) with shRNA lentiviral vectors against TF (TRCN#00000722348 and TRCN#0000431323, Sigma-Aldrich) or control shRNA vectors (Sigma-Aldrich #SHC005 and Addgene vector 1864).

qRT-PCR, Western blotting analyses, and flow cytometry

qRT-PCR was performed as described previously (9). Primer sequences are provided in Supplementary Table S2. Data are expressed as the ratio of the mRNA of interest to GAPDH and, for inducible cell lines, as fold induction in treated cells relative to the untreated ones.

For Western blotting analyses, proteins were separated on 10% SDS-PAGE and transferred to polyvinylidene difluoride membranes. The antibodies used are listed in Supplementary Table S3.

For the detection of cell surface–associated TF, cells were detached with trypsin-EDTA, labeled with a FITC-conjugated antibody against human TF (Supplementary Table S3), and analyzed with the FACSCantoII.

IHC on human samples

Human breast tissues were obtained from 40 biopsies of ductal invasive TNBCs from Reims University Hospital Biological Resource Collection no. DC-2008-374 and staged according the 2009 WHO classification. This study was approved by the Institutional Review Board of Reims University Hospital (Reims, France). Tissue sections and antigen detection were performed as described previously (see details for antibodies in Supplementary Table S3; ref. 9). The results for immunohistochemical detection of vimentin and TF were scored independently by two pathologists who had no knowledge of the clinical data, as follows: 0 = no detection; 1 = detection in <25% of tumor cells; 2 = detection in 26%–50% of tumor cells; 3 = detection in >50% of tumor cells.

Clotting assay

For the visual clotting assay, whole blood was collected from healthy donors on 3.2% sodium citrate. Cancer cells (10,000) were suspended in 600 μL of serum-free DMEM ($CaCl_2$ 1.2 mmol/L) and exposed to 300 μL of blood. Clot formation was monitored. For blocking experiments, cancer cells were pretreated with anti-TF blocking antibody (or a control IgG isotype) before the addition of whole blood (Supplementary Table S3). All clotting experiments were performed at least three times during an observation period of 4 hours. Because the clotting times varied from one blood donor to another, clot formation times from one experiment are provided as a representative example.

Mice models

All animal studies were approved by the Animal Ethics Committee of the University of Liège (Liège, Belgium). BALB/c and SCID mice (7 weeks of age) were purchased from Charles River Laboratories.

After EMT induction or si/shRNA transfection, cells (1×10^5) were injected in the tail vein. To quantify CTC persistence/early seeding or metastasis formation, mice were sacrificed 24 hours or 3–5 weeks after intravenous injection, respectively. In long-term

models, *in vivo* imaging was performed using an IVIS-200 imaging system (Xenogen Caliper) as reported previously (10) and results are expressed as the ratio of luminescence for each mouse to the mean value of the reference group (mean ± SEM). At the time of sacrifice, whole blood was collected by intracardiac puncture. To evaluate tumor cell contents in the blood and in the lungs, human GAPDH levels were quantified by RT-nested qPCR, as described previously (10). Double IHC for Ki67 and Von Willebrand Factor (VWF) were performed on paraffin section of mouse lungs, as described previously (10) and double immunofluorescence against vimentin and platelet CD42b was performed on frozen sections of mouse lungs (see details for antibodies in Supplementary Table S3).

In some experiments, enoxaparin (Clexane, Sanofi) was injected subcutaneously at 10 mg/kg one hour before cell injection as described previously (17).

CTC analysis in blood samples from breast cancer patients

The Human Ethics Committee of University of Liège approved the study protocol for CTCs, and all patients provided their written informed consent.

CTC isolation [from 22 patients with metastatic breast cancer (MBC), taken before starting a new line of anticancer therapy, and from 10 healthy donors] and analysis were performed with the ScreenCell cytokit (ScreenCell). Captured cells were fixed and permeabilized with methanol before being processed for a triple immunostaining against vimentin, TF, and cytokeratins (antibodies listed in Supplementary Table S3). The triple staining conditions were optimized using coverslip cultures of different cell lines with known status of vimentin, TF, and cytokeratin expression (Supplementary Fig. S1). Filters were scanned with Nikon eclipse Ti-S microscope. An original automatic detection program was developed in the laboratory to detect automatically "pink" signals (corresponding to pankeratin labeling). An image detection program was implemented using the image analysis toolbox of Matlab R2014a (8.3.0532) 64 bit (Mathworks, Natick) to establish colocations and therefore to enumerate CTCs expressing TF and/or vimentin. Results were validated by two independent examiners. Data were analyzed to evaluate a potential correlation between the presence of TF^+/$vimentin^+$ CTCs and overall survival from the date of the metastatic relapse (between 2010 and 2015).

Statistical analysis

Results are expressed as mean ± SEM ($n = 3$, for *in vitro* experiments) or as median with interquartile range for MBC patients. Statistical analyses were performed with Prism software (GraphPad software). *In vitro* results expressed as fold induction were analyzed with a two-tailed one-sample *t* test. *In vivo* results were analyzed with a two-tailed Mann–Whitney test. A $P < 0.05$ was considered statistically significant. Association between vimentin and TF expression in TNBCs was studied using χ^2 or Fisher exact tests. Univariate analysis was performed to evaluate the association between TF^+/$vimentin^+$ CTCs with overall survival using the Kaplan–Meier method and compared with the log-rank test.

Results

EMT-positive cells express higher levels of TF

To examine a potential link between EMT and TF, we analyzed TF expression in different cellular models of EMT. We first compared the level of TF in two well-known noninvasive, EMT-negative (EMT^-: MCF7 and T47D) and two invasive, EMT positive (EMT^+: MDA-MB-231 and Hs578T) breast tumor cell lines (Fig. 1A and B). qRT-PCR and Western blotting showed that high TF expression was restricted to EMT^+ cell lines displaying high vimentin and low E-cadherin levels (Fig. 1A and B). We next examined TF expression in three cellular models that exhibit inducible EMT after growth factor treatment: EGF-treated human mammary adenocarcinoma MDA-MB-468 cells (Fig. 1A and B; refs. 10, 30), TGFβ–treated human lung carcinoma A549 cells (9), and EGF-treated human breast tumor PMC42-LA cells (Supplementary Fig. S2A and S2B; refs. 29, 30). EMT induction was confirmed by qRT-PCR analysis and Western blotting showing vimentin overexpression and E-cadherin downregulation in all three EMT-induced cell lines (Fig. 1A and B and Supplementary Fig. S2A and S2B). Regarding TF expression, it was clearly increased both at the RNA and protein levels in all three systems induced to EMT.

Such an association between EMT and TF expression was also validated on samples of TNBCs. TNBCs were selected because of the well-described enrichment of EMT markers in this subtype (31). We thus observed that vimentin expression by cancer cells was associated with tumoral expression of TF (Fig. 1C).

EMT-positive cells display TF-dependent enhanced procoagulant activity

Because cell surface TF is determinant for coagulation, we examined cell surface–associated TF expression by flow cytometry in our cell systems (Fig. 2A). In agreement with the Western blot results, these FACS analyses revealed that the EMT^+ cells expressed more TF at the cell surface than the EMT^- cells.

Accordingly, the visual clot formation times of EMT^+ cells (MDA-MB-231 and Hs578T) were considerably shorter than those of the EMT^- cells (MCF7 and T47D; Fig. 2B). Similarly, growth factor–induced EMT^+ cells formed a clot more rapidly than their untreated controls (Fig. 2B). The visual clot formation times of the different cell lines perfectly reflected the levels of TF. Although we favored the visual clot formation assay that allowed the comparison of many conditions, we confirmed our results using thromboelastometry (ROTEM; Supplementary Fig. S2C).

Confirming the implication of EMT-induced TF expression in initiating clotting, cell incubation with a TF antibody was shown to strongly reduce clot formation in all EMT^+ cells (Supplementary Fig. S3).

EMT transcription factors modulate TF expression and coagulant properties

We further examined the potential contribution of two EMT transcription factors (ZEB1 and Snail as the prototype of the ZEB and Snail family, respectively) in the regulation of TF expression. qRT-PCR showed that ZEB1 was expressed more strongly by the EMT^+ cell lines MDA-MB-231 and Hs578T than by the EMT^- cell lines MCF7 and T47D, although this association was less clear-cut for Snail (Fig. 3A). Furthermore, both ZEB1 and Snail were induced upon growth factor induction of EMT in all 3 inducible systems (Fig. 3A and Supplementary Fig. S4A) although the induction of Snail in PMC42-LA cells treated with EGF did not reach significance.

Supporting a functional contribution of Snail and ZEB1 to TF expression, siRNA against these two transcription factors were found to drastically reduce TF protein levels both in EGF-treated

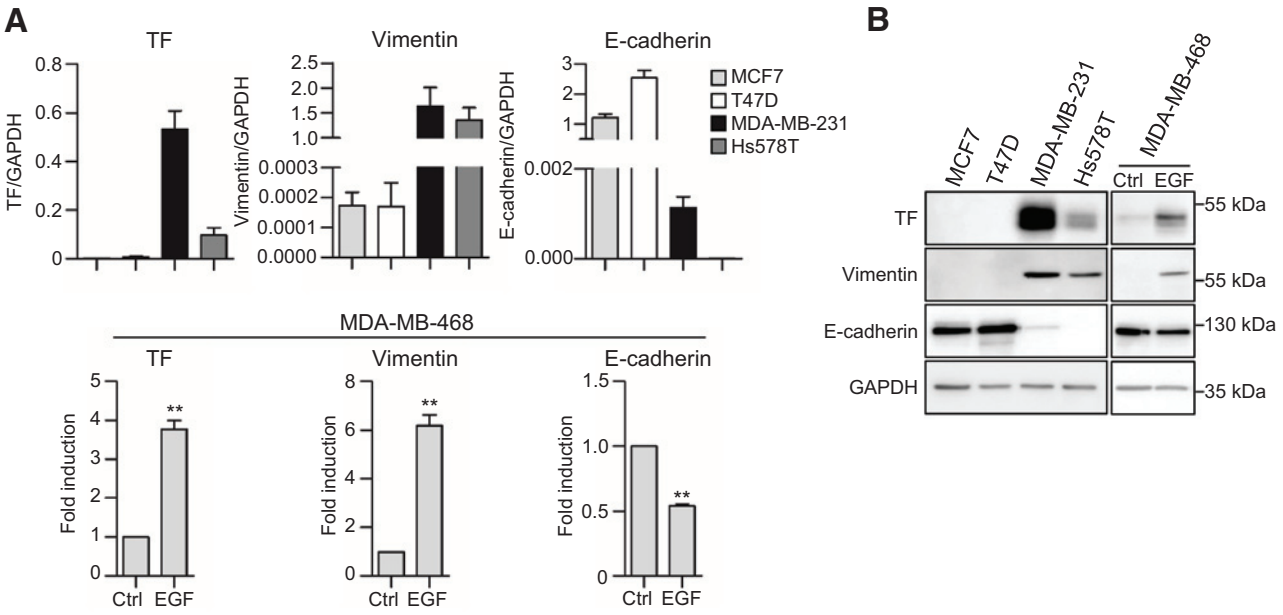

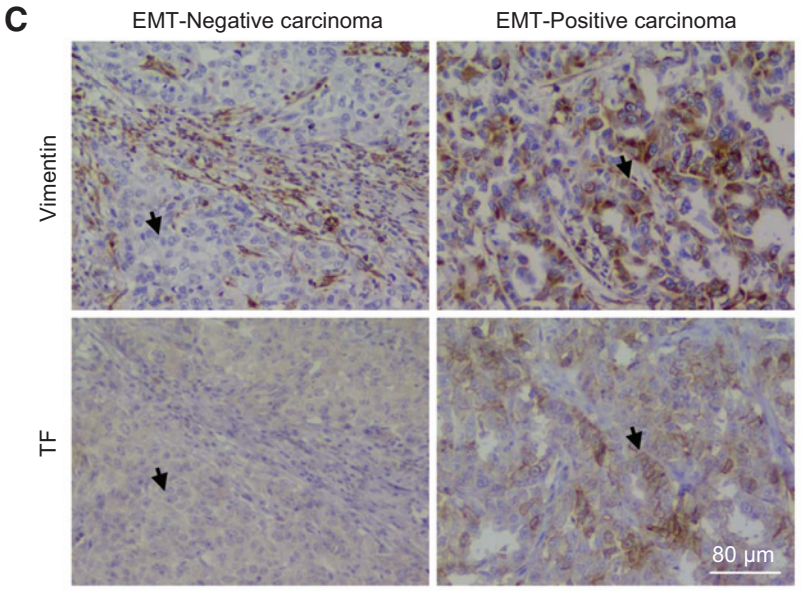

Variables	Vimentin - n=25	Vimentin + n=15	*P*
TF -	22 (85%)	4 (15%)	0.0001
TF +	3 (27%)	11 (73%)	

Figure 1.

TF expression and EMT status in different cell systems. A, qRT-PCR analyses of TF, vimentin and E-cadherin in EMT$^-$ and EMT$^+$ cell lines and in MDA-MB-468 cells not treated (Ctrl) or treated with EGF. **, $P < 0.01$. B, Western blotting analyses of TF, vimentin, and E-cadherin, and GAPDH protein as loading control. C, illustrative microscopy images of vimentin and TF staining on serial sections in TNBCs. An EMT$^-$ (left, no vimentin in tumor cells) and an EMT$^+$ (right, presence of vimentin in tumor cells) representative carcinoma are shown. Arrows, double negative or double positive tumor areas. Results of the statistical Fisher test analysis are presented.

and untreated MDA-MB-468 cells (Fig. 3B) and in the other cell systems (Supplementary Fig. S4B). Because ZEB1 silencing was stronger and was conserved in all cellular models, we focused further on the effects of ZEB1 for silencing experiments and confirmed that ZEB1 siRNA transfection inhibited clot formation using the MDA-MB-468 and MDA-MB-231 models (Fig. 3C).

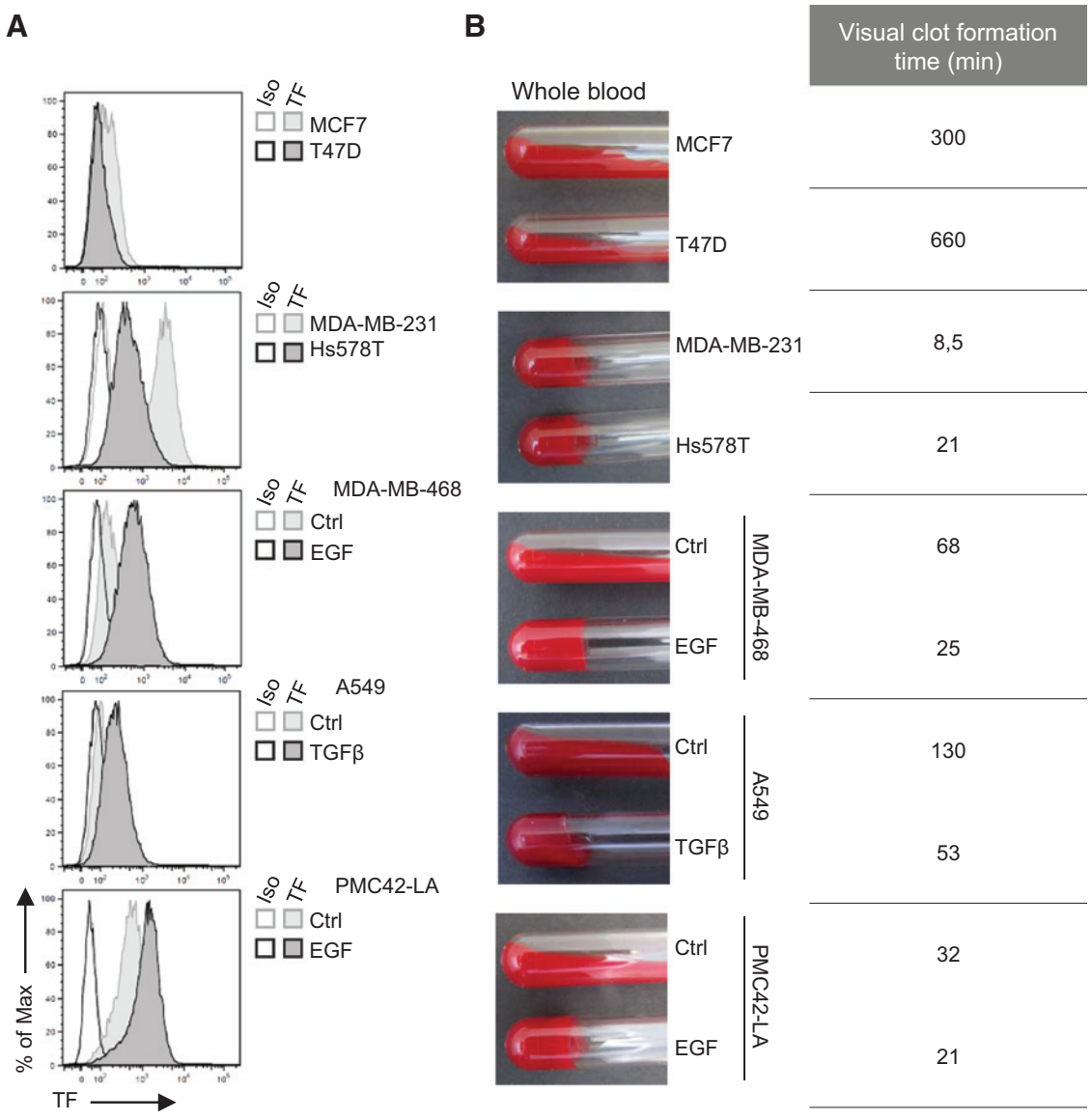

Figure 2.

Cell surface TF expression and procoagulant activity of EMT$^+$ and EMT$^-$ cell lines. A, flow cytometry analyses of surface TF expression in EMT$^-$ and EMT$^+$ cell lines and in inducible cell lines [not treated (Ctrl) or treated with EGF or TGFβ]. A corresponding isotype antibody was used as a labeling control. B, clot assays performed by incubating 10×10^3 cells with whole blood of healthy donors. Photographs were taken at a time that discriminated EMT$^+$ and EMT$^-$ cells.

Conversely, we used a model of MDA-MB-468 cells expressing a doxycycline-inducible vector for Snail (MDA-MB-468-iSnail) in which a strong expression of TF is achieved after 120 hours of doxycycline treatment, along with the induction of vimentin expression (time course presented in Supplementary Fig. S5). The induction of TF by Snail at 120 hours also associated with enhanced coagulant properties (Fig. 3D and E). Doxycycline-treatment of MDA-MB-468-iGFP control cells did not modify TF expression or the coagulant activity of the cells, showing that doxycycline treatment by itself does not modify TF expression. In addition, transfecting a siRNA against TF in the MDA-MB-468-iSnail diminished the coagulant properties induced by Snail (Fig. 3E). These results strongly suggest that the induction of coagulant properties by Snail is mediated by its impact on TF rather than on other Snail target genes.

EMT$^+$ CTCs exhibit a higher survival/persistence in colonized lungs

To examine further the impact of this identified EMT–TF regulatory axis on early metastasis of EMT$^+$ CTCs, we optimized short-term models by injecting intravenously BALB/c mice that were sacrificed 24 hours after injection. Using MDA-MB-468 and MDA-MB-231 cells, we first appraised whether EMT$^+$ cells have higher abilities to survive/seed in the colonized organs than EMT$^-$ cells, and whether this is linked to TF expression by using cells expressing a shRNA against TF that efficiently down-regulated TF protein expression and coagulant properties in

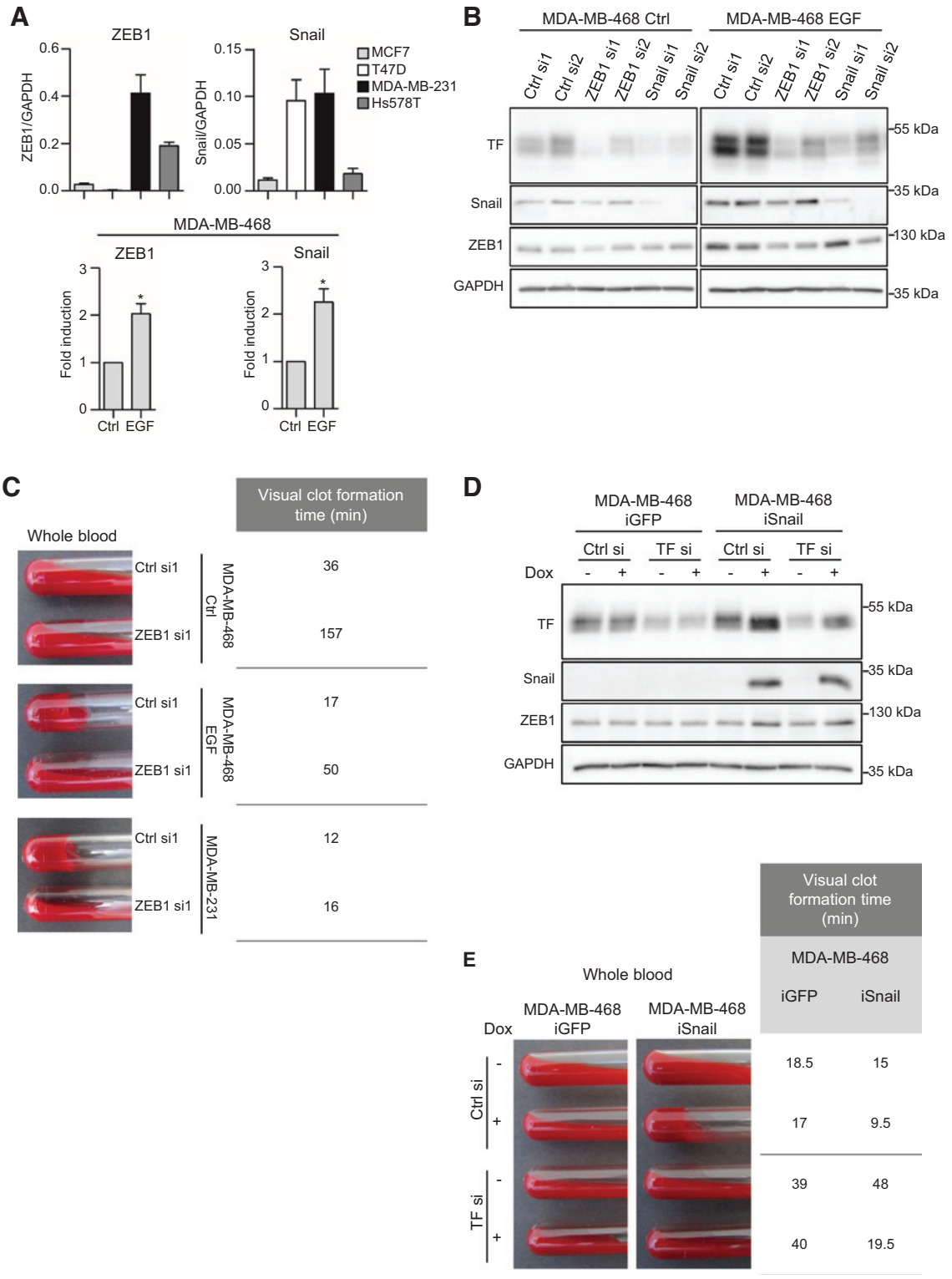

Figure 3.

Regulation of TF by EMT transcription factors. A, qRT-PCR analyses of ZEB1 and Snail in EMT^{-} and EMT^{+} cell lines and in MDA-MB-468 cells not treated (Ctrl) or treated with EGF. *, $P < 0.05$. B, Western blotting analyses of TF, Snail, and ZEB1 in MDA-MB-468 treated or not with EGF and transfected with two nontargeting siRNA (Ctrl si1 or Ctrl si2), two siRNA against ZEB1 (ZEB1 si1 or ZEB1 si2), or two siRNA against Snail (Snail si1 or Snail si2). C, clot assays performed with whole blood of healthy donors incubated with MDA-MB-468 (treated or not with EGF) and MDA-MB-231 transfected with Ctrl si1 or ZEB1 si1. D, Western blotting analyses of TF, Snail, and ZEB1. E, clot assays performed with whole blood of healthy donors incubated with MDA-MB-468 iGFP or iSnail treated or not with doxycycline (Dox) for 120 hours and transfected with Ctrl siRNA or TF siRNA.

both cell systems (Supplementary Fig. S6A and S6B). MDA-MB-468 transduced with one Ctrl sh or one TF sh were then primed with EGF treatment *in vitro* before injection. RT-nested qPCR against human GAPDH was performed to determine tumor cell content. Human GAPDH was barely detectable in the blood in all four groups of mice (data not shown), suggesting that CTCs are rapidly cleared from the circulation. In contrast, significant amounts of human GAPDH were detected in lung extracts and these levels were clearly higher in mice injected with EGF-treated MDA-MB-468 (EMT^+) transduced with Ctrl sh than in nontreated MDA-MB-468 Ctrl sh cells (EMT^-; Fig. 4A). Importantly, TF downregulation by shRNA

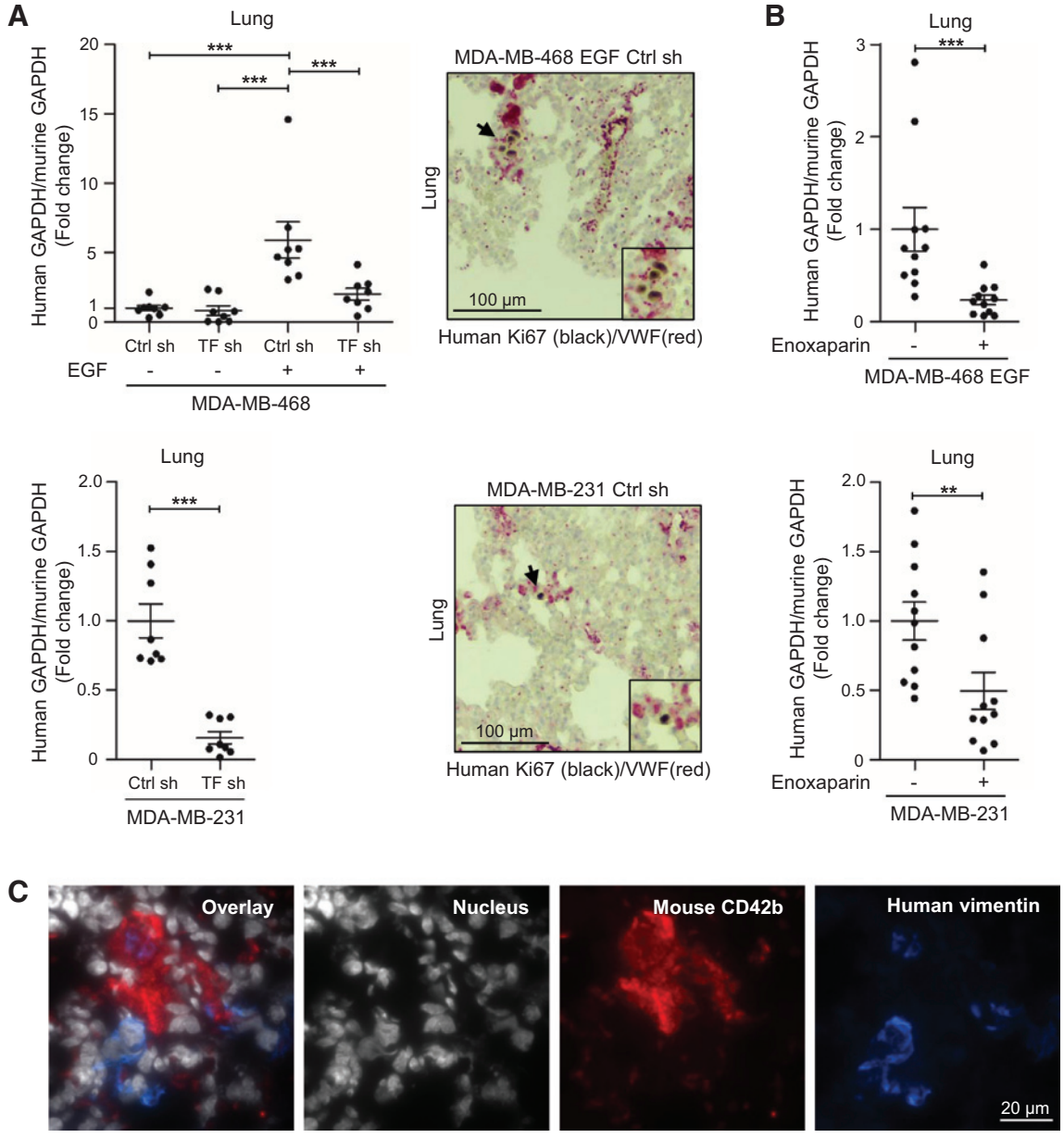

Figure 4.

Impact of TF and coagulation on CTC persistence in mouse models. A, RT-nested qPCR for human GAPDH performed on total RNA extracted from lungs of BALB/c mice injected intravenously with MDA-MB-468 cells (treated or not with EGF; $n = 8$, top) or MDA-MB-231 ($n = 8$, bottom) transduced with Ctrl shRNA or TF shRNA and collected 24 hours after injection. Double IHC against human Ki67 (black) and mouse VWF (red) performed on lung sections from mice injected with the EGF-treated MDA-MB-468 group (top) or Ctrl shRNA MDA-MB-231 group (bottom). B, RT-nested qPCR for human GAPDH performed on total RNA extracted from the lungs of BALB/c mice treated or not with 10 mg/kg of enoxaparin 1 hour before intravenous injection of EGF-treated MDA-MB-468 cells ($n = 11$, top) or MDA-MB-231 ($n = 11$, bottom). **, $P < 0.01$; ***, $P < 0.001$. C, double immunofluorescence against human vimentin (blue) and mouse CD42b (platelets, red) performed on frozen lung sections from immunodeficient mice injected with MDA-MB-231 and collected 24 hours after injection. Nuclei were labeled with TO-PRO-3 (white).

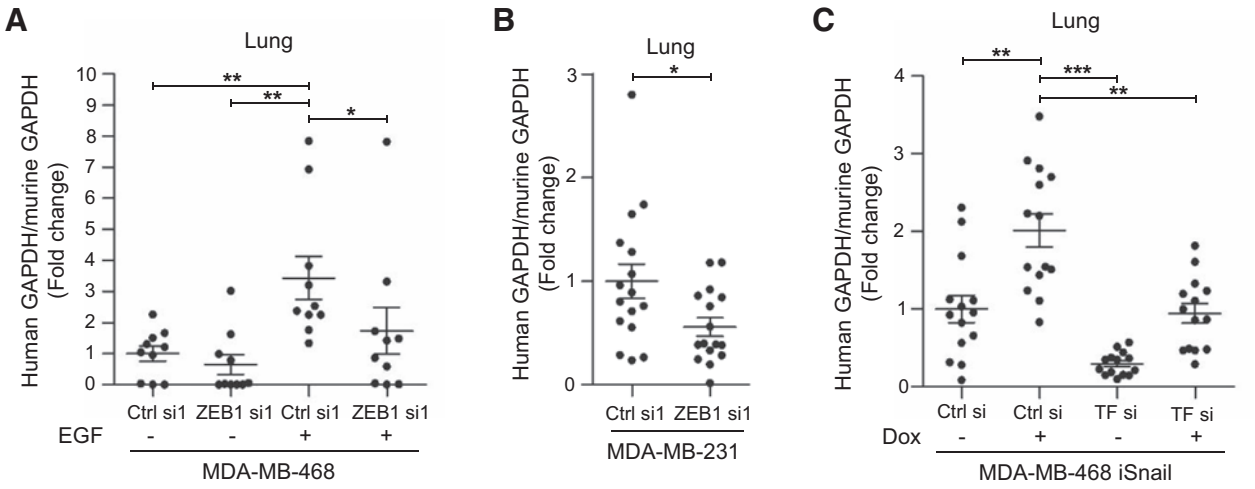

Figure 5.

CTC persistence in mice injected with cancer cell lines modulated for ZEB1 or Snail expression. RT-nested qPCR for GAPDH performed on RNA extracted from lungs of BALB/c mice injected intravenously for 24 hours with MDA-MB-468 cells (treated or not with EGF; $n = 10$; A) or MDA-MB-231 ($n = 16$) transfected with Ctrl siRNA or ZEB1 siRNA (B) or MDA-MB-468 iSnail (treated or not with doxycycline) transfected with Ctrl siRNA or TF siRNA ($n = 14$; C). *, $P < 0.05$; **, $P < 0.01$; ***, $P < 0.001$. Dox, doxycycline.

significantly abrogated the observed increased cell persistence associated with the induction of EMT by EGF. IHC against human Ki67 (black) and mouse VWF (red) qualitatively confirmed the presence of isolated tumor cells in the pulmonary microvasculature and parenchyma of mice injected with EGF-treated Ctrl sh (Fig. 4A). Similar results were obtained with MDA-MB-231 cells (Fig. 4A). These results thus showed that EMT^+ cells have the ability to undertake the early steps of metastases (i.e., survival and early seeding) and implicate TF in such properties.

Clearly implicating coagulation in these early metastatic processes, a significant decrease in tumor cell content was observed in the lungs of mice pretreated with the anticoagulant enoxaparin and then injected with EGF-treated MDA-MB-468 or MDA-MB-231 (Fig. 4B). Also, double immunofluorescence against mouse CD42b (a platelet marker) and human vimentin revealed that MDA-MB-231 cells colonizing the lungs were surrounded by platelet-rich microthrombi (Fig. 4C) and transmission electron microscopy further evidenced the presence of fibrin fibers around these colonizing cells (Supplementary Fig. S7).

Strengthening the link between EMT, the TF/coagulation axis, and early metastatic colonization, ZEB1 silencing was clearly shown to diminish cell persistence both of EGF-induced MDA-MB-468 cells (Fig. 5A) and of MDA-MB-231 (Fig. 5B). Furthermore, using the MDA-MB-468-iSnail system demonstrated a higher persistence in the lungs of the doxycycline-induced cells expressing Snail than the untreated cells (Fig. 5C). The transfection of a siRNA against TF diminished this Snail-induced persistence in the lungs (Fig. 3E), confirming the implication of Snail-induced TF in this process and not other Snail target genes.

These data taken together thus support the involvement of TF-dependent and coagulation-dependent mechanisms in early metastatic colonization of EMT^+ tumor cells.

To confirm the ability of seeded cells to develop metastasis, we examined further the impact of EMT and TF modifications on overall long-term metastasis formation. The luciferase-expressing MDA-MB-231 cells silenced for TF or ZEB1 were thus intravenously injected in SCID mice for 3–5 weeks to allow metastatic growth. We observed that mice injected with control cells showed a higher level of luciferase activity both *in toto* and in the dissected lungs compared with mice injected with cells silenced for TF or ZEB1 (Fig. 6A and D). RT-nested qPCR for human GAPDH corroborated these observations (Fig. 6B and E). IHC for human Ki67 confirmed the presence of lung metastases in the control group while smaller and fewer metastases were observed in the TF or ZEB1-silenced groups (Fig. 6C and F). These results obtained with long-term mouse models are in agreement with independent literature showing the involvement of ZEB1 (6, 8) and TF on metastasis development (13).

CTCs expressing vimentin and TF are present in the blood samples of MBC patients

To provide clinical validation of our *in vitro* and animal observations, we looked for TF/vimentin expressing CTCs in the blood of MBC patients. Patient details are provided in Supplementary Table S4. Because of the known limitations in using existing immunomagnetic isolation method based on the epithelial cell surface antigen to analyze EMT-derived CTCs (32), we used ScreenCell filtration devices to enrich CTCs and performed a triple immunofluorescent labeling (pan-keratins, TF, vimentin). Some cells strongly expressing keratins but not TF or vimentin were found at a similar level both in healthy donors and cancer patients that could represent circulating epithelial cells. In contrast, keratin-positive cells expressing TF, vimentin, or both were found only in cancer patients and not in healthy donors, and were enumerated. Representative images of these three CTC phenotypes present in blood samples of MBC patients are shown in Fig. 7A. Most interestingly, a population of CTCs expressing cytokeratins and both TF and vimentin was identified in 19 of 22 (86.3%) patients. A CTC population expressing cytokeratins and TF but no detectable vimentin was also found in 81.8% of the cancer patients. In contrast, CTCs expressing cytokeratins and only vimentin represented a rare population found only in 9 patients

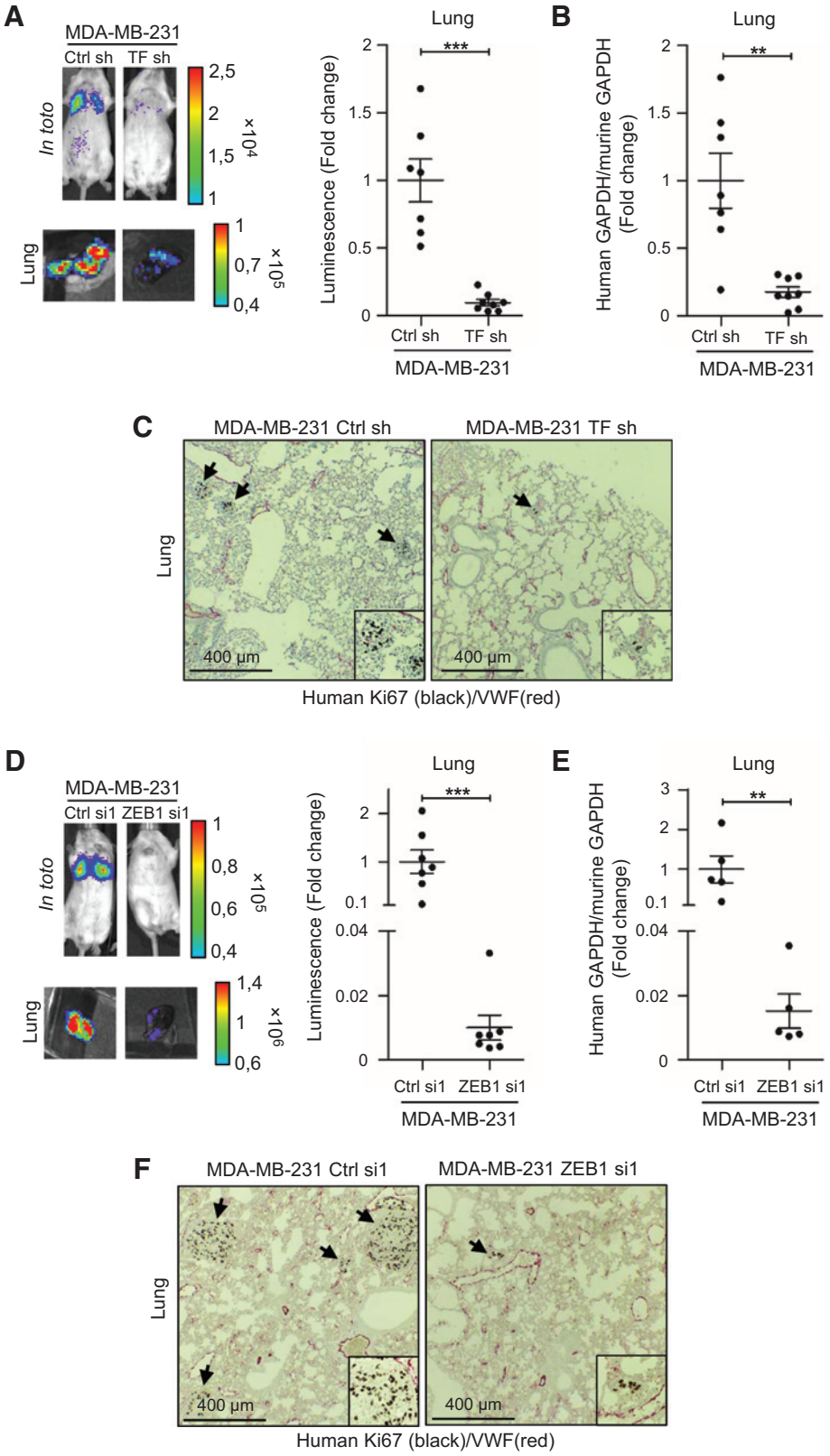

Figure 6.

Metastasis formation in SCID mice injected with MDA-MB-231 silenced for TF (A–C) or ZEB1 (D–F) expression. A and D, *In vivo* imaging analyses of SCID mice injected intravenously with MDA-MB-231 cells 3–5 weeks after injections, and of collected lungs ($n = 7$). B and E, RT-nested qPCR for human GAPDH performed on total RNA extracted from lungs ($n = 7$ for B and $n = 5$ for E). **, $P < 0.01$; ***, $P < 0.001$. C and F, double IHC against human Ki67 (black) and mouse VWF (red) performed on lung sections. Arrows, metastatic foci.

(40.9%; Fig. 7B and C). Although a large-scale study is needed to refine the clinical value of this subpopulation of CTCs, it is interesting to note that the presence of TF^+/vimentin$^+$ CTCs correlated with a shorter survival. The highest significance ($P = 0.039$) was observed with a cut-off point at 3 TF^+/vimentin$^+$ CTCs (Fig. 7D).

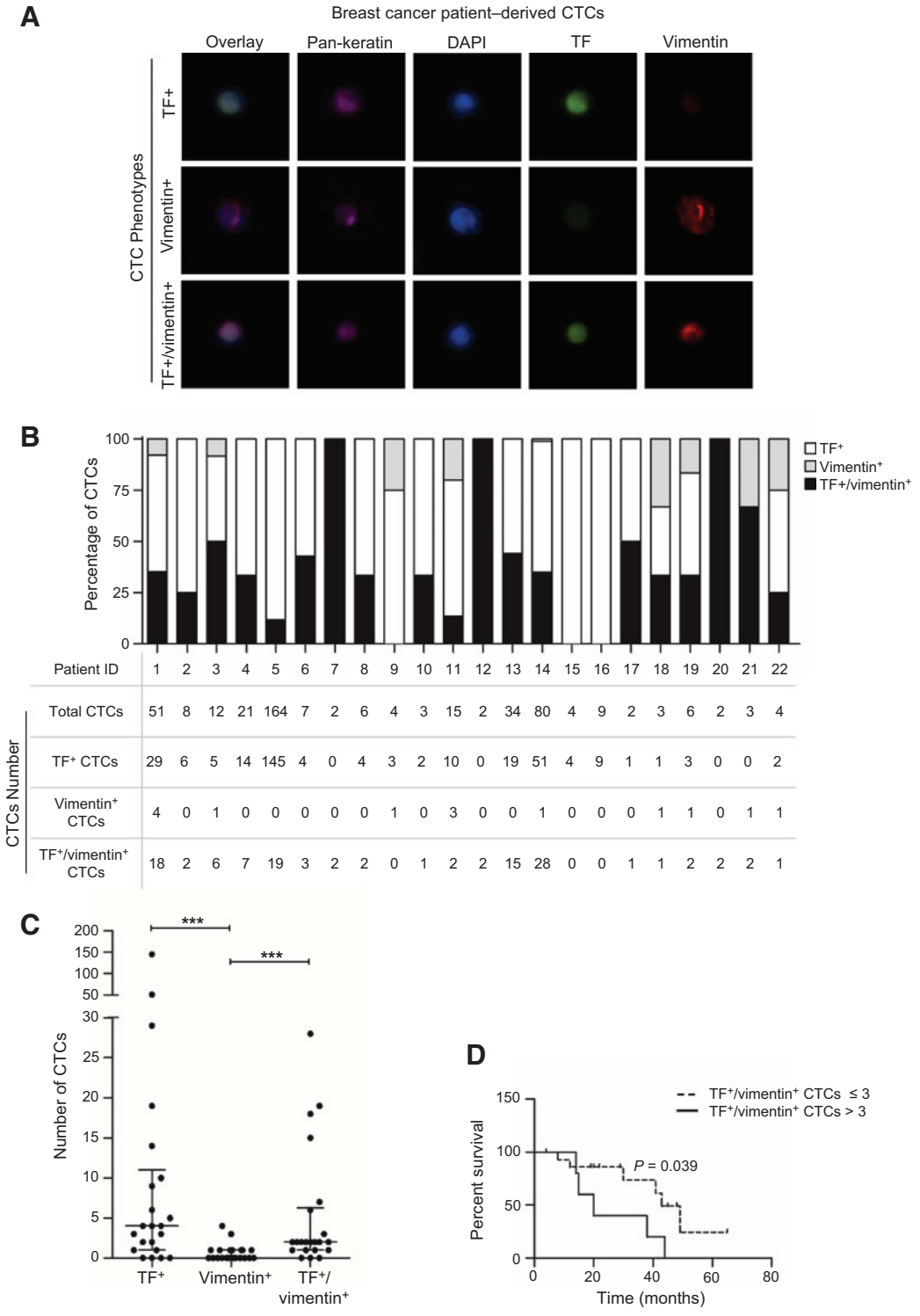

Figure 7.

TF and vimentin expression in CTCs isolated from MBC patients. A, representative images of the triple immunostaining performed on ScreenCell filters showing the CTC phenotypes found in MBC patients (pan-keratin, pink; TF, green; vimentin, red; DAPI, blue). B, quantitation of CTC phenotypes in each patient. C, graph plot of CTC numbers found in MBC patients as a function of their phenotype (CTCs expressing only TF, only vimentin, or both). ***, $P < 0.001$. D, association between TF^+/$vimentin^+$ CTCs and overall survival of MBC patients (cut-off point at 3 TF^+/$vimentin^+$ CTCs, Kaplan–Meier method with log-rank test).

Discussion

We provide evidence that an EMT-induced pathway leading to the overexpression of TF and corresponding procoagulant properties contributes to the persistence/early metastatic colonization of CTCs.

Despite early independent implications of both in carcinoma metastasis, the link between EMT and TF has been largely unappreciated. Here TF was found to be overexpressed in association with EMT in three different growth factor EMT-inducible cell systems, and TF expression was highest in the invasive, EMT^+ MDA-MB-231 and Hs578T breast cancer cell lines. Strengthening this EMT–TF axis, we further report the modulation of TF expression by well-known EMT transcription factors ZEB1 and Snail. In support of our observations, Rak and colleagues reported enhanced TF expression and release of TF-containing microparticles from human A431 cervical cancer cells induced to EMT through EGFR activation or E-cadherin blockade. They showed that xenografts of A431 cells also release TF into the bloodstream and enhance overall coagulopathy compared with tumor-free mice (33–35). Our data correlating vimentin and TF expression in the biopsies of TNBCs further emphasizes a link between EMT and TF expression in human tumor tissues. Most importantly, we were able to validate this association between vimentin and TF expression in a subpopulation of CTCs of MBC patients. If such a TF^+/$vimentin^+$ phenotype is seen in tumors, it could also be acquired in the bloodstream. Accordingly, platelets have been reported to induce EMT and TF expression in different types of cancer cells (36, 37).

We further implicate this identified EMT–TF axis in early metastasis of CTCs. Our data indeed show that EMT-induced TF provides CTCs with enhanced survival/early seeding properties. The observation that EMT-induced cells silenced for TF or ZEB1 were less persistent in the lungs of intravenously injected mice and that doxycycline-induced cells expressing Snail were more persistent in the lungs of intravenously injected mice clearly supports a causal role of EMT-induced TF in these early metastatic processes. Corroborating these *in vivo* findings, shRNA/siRNA against TF or TF-blocking antibodies strongly diminished the EMT-induced *in vitro* procoagulant activity in all cellular models examined. Our findings showing that the anticoagulant molecule enoxaparin decreased EMT^+ cell persistence in the lungs, further confirmed the implication of the coagulation system in the process.

Although the impact of such EMT/TF axis on early metastatic steps has never been reported, our data are generally supported by reports demonstrating that TF favors metastasis. Targeting TF or TF pathway with TF-antibodies or TF inhibitors accordingly represents today a promising alternative therapeutic strategy for cancer patients to the use of global anticoagulants, the routine use of which is often associated with bleeding complications (26, 38–40). Thus, the administration of TF-blocking antibodies in experimental metastases models was shown to reduce short-term persistence in colonized organs of B16 melanoma cells (39) or of human pancreatic cancer cell lines BxPCR3 (41), as well as the development of metastases by these two cell lines or MDA-MB-231 cells (40). Similarly, siRNA against TF decreased lung metastatic burden from intravenous-injected B16 melanoma cells or from xenografts of human melanoma cells (42), while overexpression of different TF constructs in human melanoma cells enhanced the development of lung metastases in intravenously injected SCID mice (43). Using mutant constructs of TF that are unable to initiate the coagulation cascade, these authors further revealed the importance of noncoagulant functions of TF in metastatic growth (43). On the other hand, coagulation-dependent effects of TF on metastases have been demonstrated by the laboratory of J.L. Degen (Cincinnati Children's Hospital Medical Center, Cincinnati, OH), who injected intravenously tumor cells modified for TF expression in mice with genetic defects in distal hemostatic factors (prothrombin and fibrinogen). They thus revealed that TF supports metastasis through mechanisms dependent on these distal hemostatic factors (13, 21).

Taken together, these observations suggest that both coagulation-dependent and independent functions of TF therefore contribute to the metastatic development, depending on the cellular and mice models used, whereas coagulation-dependent functions would more selectively support early metastatic steps. Such conclusions are also supported by our results obtained with the enoxaparin-treated mice and by literature similarly reporting the beneficial impact of anticoagulants (15, 16) or of mice deficient for distal hemostatic factors (such as fibrinogen; ref. 44) in short-term experimental metastasis models using B16 or LLC cells.

The precise mechanisms by which coagulation events may favor early persistence of CTCs in the colonized organs remain elusive. Examining colonizing MDA-MB-231 cells 24 hours after intravenous injection, we showed that cells are covered with platelets and the presence of fibrin fibers around the cells was evidenced by transmission electron microscopy, supporting the idea of the formation of a "protective cocoon" as proposed in early work (19). In the light of the importance of CTC-associated TF expression, it is possible that a local activation of the coagulation cascade around CTCs plays a major role in the formation of such a fibrin-rich pericellular network. This network could protect CTCs against hostile signals including shear stress, modifications of cell–cell and cell–matrix interactions, or immune cells, and would promote their metastatic potential. A mechanism involving a protective role of fibrin and/or platelets in NK-induced cytotoxicity against tumor cells has, for instance, been demonstrated *in vitro* and using NK-deficient mice in experimental metastasis assays by Degen and colleagues (21, 44–48). On the other hand, NK-independent processes have also been evidenced (21), one of which implicates the recruitment of monocytes/macrophages in microthrombi favoring the establishment of so-called premetastatic niches (49).

Interestingly, a new insight in the CTC field is the identification of CTC clusters within the circulation and, which, although much less prevalent than isolated CTCs, have been suggested to have high metastatic potential (50). In the light of our results, it is tempting to speculate that coagulation events could be implicated in the formation or persistence of these clusters. Literature reporting xenografts in animal models has suggested that CTC clusters arise from the fragmenting of primary tumor cell clumps rather than from intravascular aggregation of single CTCs (50). Accordingly, in our experimental metastasis models, colonizing EMT^+ cells in the lungs were rarely observed as clusters. In our samples of CTCs isolated from MBC patients, CTC clusters were actually only occasionally observed. A study by Yu and colleagues, nevertheless reported that breast CTCs expressing EMT traits occurred predominantly as single cells but also as multicellular clusters surrounded by platelets (12). Though TF expression was not examined in this study; this latter observation is in direct relationship with our results and supports the idea that blood components could also play a role in the survival of these clusters. Nevertheless, the data to establish the potential implication of coagulation in the

formation or survival of CTC clusters are still preliminary and warrant further investigation.

Taken together, our data show that TF expression is upregulated during EMT, providing tumor cells with enhanced coagulant properties that facilitate early steps of their metastatic colonization. Emphasizing the clinical relevance of our observations and the importance of EMT in the CTC compartment, we identified CTCs expressing both vimentin and TF in 86.3% of MBC patients while CTCs expressing only vimentin but not TF were very rare. Our data thus support a mechanism by which a local activation of coagulation triggered by enhanced TF expression could trap EMT^+ CTCs in platelet/fibrin-microthrombi, thereby favoring their survival and early seeding in colonized organs. Targeting such a local mechanism could represent an important extension to global anticoagulant strategies against cancer.

Disclosure of Potential Conflicts of Interest

No potential conflicts of interest were disclosed.

Authors' Contributions

Conception and design: M. Bourcy, G. Jerusalem, C. Gilles
Development of methodology: M. Bourcy, M. Suarez-Carmona, J. Lambert, M.-E. Francart, C. Delierneux, S. Blacher, C. Oury, C. Gilles
Acquisition of data (provided animals, acquired and managed patients, provided facilities, etc.): M. Bourcy, H. Schroeder, N. Skrypek, G. Jerusalem, G. Berx, M. Thiry, S. Blacher, C. Gilles
Analysis and interpretation of data (e.g., statistical analysis, biostatistics, computational analysis): M. Bourcy, M. Suarez-Carmona, N. Skrypek, G. Berx, M. Thiry, S. Blacher, A. Noel, C. Oury, M. Polette, C. Gilles
Writing, review, and/or revision of the manuscript: M. Bourcy, E.W. Thompson, G. Jerusalem, B.G. Hollier, A. Noel, C. Oury, M. Polette, C. Gilles
Administrative, technical, or material support (i.e., reporting or organizing data, constructing databases): M. Bourcy, H. Schroeder, B.G. Hollier, C. Gilles
Study supervision: M. Bourcy, M. Polette, C. Gilles

Acknowledgments

The authors thank Erika Konradowski, Marie Dehuy, Nathalie Lefin, Emilie Feyereisen, Isabelle Dasoul, Patricia Piscicelli, Laure Volders, and Guy Roland for technical assistance and Dr. Thomas Westbrook for the pINDUCER20 construct (Verna & Marrs McLean Department of Biochemistry & Molecular Biology, Baylor College of Medicine, Houston, TX). The authors also thank the following technical platforms from the University of Liège (Liège, Belgium): GIGA-Viral vectors Platform for viral particles productions, the GIGA-imaging and flow cytometry platform for providing access to FACSCanto II (BD Biosciences), and the GIGA-Animal Facility.

Grant Support

This work was supported by grants from the "Fonds de la Recherche Scientifique" (F.R.S.-FNRS, Belgium), the "Fondation contre le Cancer", the "Partenariat Hubert Curien-Tournesol", the "Fonds spéciaux de la Recherche" (University of Liège), the "Centre Anticancéreux près l'Université de Liège", the "Fonds Léon Fredericq" (University of Liège), the "Direction Générale Opérationnelle de l'Economie", de l'Emploi et de la Recherche from the Service Public de Wallonie (SPW, Belgium), the Interuniversity Attraction Poles Programme (Brussels, Belgium), the "Actions de Recherche Concertées" (University of Liège, Belgium; to C. Gilles, A. Noël, and C. Oury). B.G. Hollier is supported by grants from the Australian Government Department of Health, the Movember Foundation and Prostate Cancer Foundation of Australia through a Movember Revolutionary Team Award. E.W. Thompson was supported in part by the National Breast Cancer Foundation (Australia).

The costs of publication of this article were defrayed in part by the payment of page charges. This article must therefore be hereby marked *advertisement* in accordance with 18 U.S.C. Section 1734 solely to indicate this fact.

Received August 17, 2015; revised March 16, 2016; accepted April 26, 2016; published OnlineFirst May 24, 2016.

References

1. McInnes LM, Jacobson N, Redfern A, Dowling A, Thompson EW, Saunders CM. Clinical implications of circulating tumor cells of breast cancer patients: role of epithelial-mesenchymal plasticity. Front Oncol 2015;5:42.
2. Pantel K, Speicher MR. The biology of circulating tumor cells. Oncogene 2016;35:1216–24.
3. Toss A, Mu Z, Fernandez S, Cristofanilli M. CTC enumeration and characterization : moving toward personalized medicine. Ann Transl Med 2014;2:108.
4. Bonnomet A, Brysse A, Tachsidis A, Waltham M, Thompson EW, Polette M, et al. Epithelial-to-mesenchymal transitions and circulating tumor cells. J Mammary Gland Biol Neoplasia 2010;15:261–73.
5. Krawczyk N, Meier-stiegen F, Banys M, Neubauer H, Ruckhaeberle E, Fehm T. Expression of stem cell and epithelial-mesenchymal transition markers in circulating tumor cells of breast cancer patients. Biomed Res Int 2014;2014:415721.
6. De Craene B, Berx G. Regulatory networks defining EMT during cancer initiation and progression. Nat Rev Cancer 2013;13:97–110.
7. Nieto MA, Cano A. The epithelial-mesenchymal transition under control: global programs to regulate epithelial plasticity. Semin Cancer Biol 2012;22:361–8.
8. Puisieux A, Brabletz T, Caramel J. Oncogenic roles of EMT-inducing transcription factors. Nat Cell Biol 2014;16:488–94.
9. Suarez-Carmona M, Bourcy M, Lesage J, Leroi N, Syne L, Blacher S, et al. Soluble factors regulated by epithelial-mesenchymal transition mediate tumour angiogenesis and myeloid cell recruitment. J Pathol 2015;236:491–504.
10. Bonnomet A, Syne L, Brysse A, Feyereisen E, Thompson EW, Noël A, et al. A dynamic in vivo model of epithelial-to-mesenchymal transitions in circulating tumor cells and metastases of breast cancer. Oncogene 2012;31:3741–53.
11. Aktas B, Tewes M, Fehm T, Hauch S, Kimmig R, Kasimir-Bauer S. Stem cell and epithelial-mesenchymal transition markers are frequently overexpressed in circulating tumor cells of metastatic breast cancer patients. Breast Cancer Res 2009;11:R46.
12. Yu M, Bardia A, Wittner BS, Stott SL, Smas ME, Ting DT, et al. Circulating breast tumor cells exhibit dynamic changes in epithelial and mesenchymal composition. Science 2013;339:580–4.
13. Palumbo JS, Degen JL. Mechanisms linking tumor cell-associated procoagulant function to tumor metastasis. ThrombRes 2007;120:S22–8.
14. Gil-Bernabé AM, Lucotti S, Muschel RJ. Coagulation and metastasis: what does the experimental literature tell us? Br J Haematol 2013;162:433–41.
15. Esumi N, Fan D, Fidler IJ. Inhibition of murine melanoma experimental metastasis by recombinant desulfatohirudin, a highly specific thrombin inhibitor. Cancer Res 1991;51:4549–56.
16. Hu L, Lee M, Campbell W, Perez-Soler R, Karpatkin S. Role of endogenous thrombin in tumor implantation, seeding, and spontaneous metastasis. Blood 2004;104:2746–51.
17. Mousa SA, Linhardt R, Francis JL, Amirkhosravi A. Anti-metastatic effect of a non-anticoagulant low-molecular-weight heparin versus the standard low-molecular-weight heparin, enoxaparin. Thromb Haemost 2006;96:816–21.
18. Lee AY. Thrombosis in cancer: an update on prevention, treatment, and survival benefits of anticoagulants. Hematology Am Soc Hematol Educ Program 2010;2010:144–9.
19. Crissman JD, Hatfield JS, Menter DG, Sloane B, Honn KV. Morphological study of the interaction of intravascular tumor cells with endothelial cells and subendothelial matrix. Cancer Res 1988;48:4065–72.
20. Im JH, Fu W, Wang H, Bhatia SK, Hammer DA, Kowalska MA, et al. Coagulation facilitates tumor cell spreading in the pulmonary vasculature during early metastatic colony formation. Cancer Res 2004;64:8613–9.

21. Palumbo JS, Talmage KE, Massari JV, La Jeunesse CM, Flick MJ, Kombrinck KW, et al. Tumor cell-associated tissue factor and circulating hemostatic factors cooperate to increase metastatic potential through natural killer cell-dependent and -independent mechanisms. Blood 2007;110:133–41.
22. Ruf W. Tissue factor and cancer. Thromb Res 2012;130:S84–7.
23. Ünlü B, Versteeg HH. Effects of tumor-expressed coagulation factors on cancer progression and venous thrombosis: is there a key factor? Thromb Res 2014;133:S76–84.
24. Magnus N, D'Asti E, Meehan B, Garnier D, Rak J. Oncogenes and the coagulation system – forces that modulate dormant and aggressive states in cancer. Thromb Res 2014;133:S1–9.
25. Williams JC, Mackman N. Tissue factor in health and disease. Front Biosci 2012;4:358–72.
26. Cole M, Bromberg M. Tissue factor as a novel target for treatment of breast cancer. Oncologist 2013;18:14–8.
27. Rautou PE, Mackman N. Microvesicles as risk markers for venous thrombosis. Expert Rev Hematol 2013;6:91–101.
28. Åberg M, Siegbahn A. Tissue factor non-coagulant signaling - molecular mechanisms and biological consequences with a focus on cell migration and apoptosis. J Thromb Haemost 2013;11:817–25.
29. Ackland ML, Newgreen DF, Fridman M, Waltham MC, Arvanitis A, Minichiello J, et al. Epidermal growth factor-induced epithelio-mesenchymal transition in human breast carcinoma cells. Lab Invest 2003; 83:435–48.
30. Cursons J, Leuchowius KJ, Waltham M, Tomaskovic-Crook E, Foroutan M, Bracken CP, et al. Stimulus-dependent differences in signalling regulate epithelial-mesenchymal plasticity and change the effects of drugs in breast cancer cell lines. Cell Commun Signal 2015;13:26.
31. Jeong H, Ryu YJ, An J, Lee Y, Kim A. Epithelial-mesenchymal transition in breast cancer correlates with high histological grade and triple-negative phenotype. Histopathology 2012;60:E87–95.
32. Alix-Panabières C, Pantel K. Technologies for detection of circulating tumor cells: facts and vision. Lab Chip 2014;14:57–62.
33. Milsom CC, Yu JL, Mackman N, Micallef J, Anderson GM, Guha A, et al. Tissue factor regulation by epidermal growth factor receptor and epithelial-to-mesenchymal transitions: effect on tumor initiation and angiogenesis. Cancer Res 2008;68:10068–76.
34. Garnier D, Magnus N, Lee TH, Bentley V, Meehan B, Milsom C, et al. Cancer cells induced to express mesenchymal phenotype release exosome-like extracellular vesicles carrying tissue factor. J Biol Chem 2012;287: 43565–72.
35. Garnier D, Milsom C, Magnus N, Meehan B, Weitz J, Yu J, et al. Role of the tissue factor pathway in the biology of tumor initiating cells. Thromb Res 2010;125:S44–50.
36. Orellana R, Kato S, Erices R, Bravo ML, Gonzalez P, Oliva B, et al. Platelets enhance tissue factor protein and metastasis initiating cell markers, and act as chemoattractants increasing the migration of ovarian cancer cells. BMC Cancer 2015;15:290.
37. Labelle M, Begum S, Hynes RO. Platelets guide the formation of early metastatic niches. Proc Natl Acad Sci U S A 2014;111:E3053–61.
38. Breij EC, De Goeij BE, Verploegen S, Schuurhuis DH, Amirkhosravi A, Francis J, et al. An antibody – drug conjugate that targets tissue factor exhibits potent therapeutic activity against a broad range of solid tumors. Cancer Res 2014;74:1214–26.
39. Mueller BM, Reisfeld RA, Edgington TS, Ruf W. Expression of tissue factor by melanoma cells promotes efficient hematogenous metastasis. Proc Natl Acad Sci U S A 1992;89:11832–6.
40. Ngo CV, Picha K, McCabe F, Millar H, Tawadros R, Tam SH, et al. CNTO 859, a humanized anti-tissue factor monoclonal antibody, is a potent inhibitor of breast cancer metastasis and tumor growth in xenograft models. Int J Cancer 2007;120:1261–7.
41. Saito Y, Hashimoto Y, Kuroda J, Yasunaga M, Koga Y, Takahashi A, et al. The inhibition of pancreatic cancer invasion-metastasis cascade in both cellular signal and blood coagulation cascade of tissue factor by its neutralisation antibody. Eur J Cancer 2011;47:2230–9.
42. Amarzguioui M, Peng Q, Wiiger MT, Vasovic V, Babaie E, Holen T, et al. *Ex vivo* and *in vivo* delivery of anti-tissue factor short interfering RNA inhibits mouse pulmonary metastasis of B16 melanoma cells. Clin Cancer Res 2006;12:4055–61.
43. Bromberg ME, Konigsberg WH, Madison JF, Pawashe A, Garen A. Tissue factor promotes melanoma metastasis by a pathway independent of blood coagulation. Proc Natl Acad Sci U S A 1995;92:8205–9.
44. Palumbo JS, Kombrinck KW, Drew AF, Grimes TS, Kiser JH, Degen JL, et al. Fibrinogen is an important determinant of the metastatic potential of circulating tumor cells. Blood 2000;96:3302–9.
45. Nieswandt B, Hafner M, Echtenacher B, Männel DN. Lysis of tumor cells by natural killer cells in mice is impeded by platelets. Cancer Res 1999;59: 1295–300.
46. Palumbo JS, Talmage KE, Massari JV, La Jeunesse CM, Flick MJ, Kombrinck KW, et al. Platelets and fibrin(ogen) increase metastatic potential by impeding natural killer cell-mediated elimination of tumor cells. Blood 2005;105:178–85.
47. Biggerstaff JP, Seth N, Amirkhosravi A, Amaya M, Fogarty S, Meyer TV, et al. Soluble fibrin augments platelet/tumor cell adherence in vitro and in vivo, and enhances experimental metastasis. Clin Exp Metastasis 1999;17:723–30.
48. Gorelik E, Bere WW, Herberman RB. Role of NK cells in the antimetastatic effect of anticoagulant drugs. Int J Cancer 1984;33:87–94.
49. Gil-Bernabé AM, Ferjancic S, Tlalka M, Zhao L, Allen PD, Im JH, et al. Recruitment of monocytes/macrophages by tissue factor-mediated coagulation is essential for metastatic cell survival and premetastatic niche establishment in mice. Blood 2012;119:3164–75.
50. Aceto N, Toner M, Maheswaran S, Haber DA. En route to metastasis: circulating tumor cell clusters and epithelial-to- mesenchymal transition. Trends Cancer 2015;1:44–52.